

## MEASURING THE HADRONIC CROSS SECTION AT KLOE USING THE RADIATIVE RETURN

### The KLOE Collaboration:

A. Aloisio<sup>g</sup>, F. Ambrosino<sup>g</sup>, A. Antonelli<sup>c</sup>, M. Antonelli<sup>c</sup>, C. Bacci<sup>l</sup>, G. Barbiellini<sup>n</sup>,  
F. Bellini<sup>l</sup>, G. Bencivenni<sup>c</sup>, S. Bertolucci<sup>c</sup>, C. Bini<sup>j</sup>, C. Bloise<sup>c</sup>, V. Bocci<sup>j</sup>, F. Bossi<sup>c</sup>,  
P. Branchini<sup>l</sup>, S. A. Bulychjov<sup>f</sup>, G. Cabibbo<sup>j</sup>, R. Caloi<sup>j</sup>, P. Campana<sup>c</sup>, G. Capon<sup>c</sup>, G. Carboni<sup>k</sup>,  
M. Casarsa<sup>n</sup>, V. Casavola<sup>e</sup>, G. Cataldi<sup>e</sup>, F. Ceradini<sup>l</sup>, F. Cervelli<sup>h</sup>, F. Cevenini<sup>g</sup>, G. Chiefari<sup>g</sup>,  
P. Ciambrone<sup>c</sup>, S. Conetti<sup>o</sup>, E. De Lucia<sup>j</sup>, G. De Robertis<sup>a</sup>, P. De Simone<sup>c</sup>, G. De Zorzi<sup>j</sup>,  
S. Dell'Agnello<sup>c</sup>, A. Denig<sup>c</sup>, A. Di Domenico<sup>j</sup>, C. Di Donato<sup>g</sup>, S. Di Falco<sup>d</sup>, A. Doria<sup>g</sup>,  
M. Dreucci<sup>c</sup>, O. Erriquez<sup>a</sup>, A. Farilla<sup>l</sup>, G. Felici<sup>c</sup>, A. Ferrari<sup>l</sup>, M. L. Ferrer<sup>c</sup>, G. Finocchiaro<sup>c</sup>,  
C. Forti<sup>c</sup>, A. Franceschi<sup>c</sup>, P. Franzini<sup>c,j</sup>, C. Gatti<sup>h</sup>, P. Gauzzi<sup>j</sup>, A. Giannasi<sup>h</sup>, S. Giovannella<sup>c</sup>,  
E. Gorini<sup>e</sup>, F. Grancagnolo<sup>e</sup>, E. Graziani<sup>l</sup>, S. W. Han<sup>b,c</sup>, M. Incagli<sup>h</sup>, L. Ingrosso<sup>c</sup>, W. Kluge<sup>d</sup>,  
C. Kuo<sup>d</sup>, V. Kulikov<sup>f</sup>, F. Lacava<sup>j</sup>, G. Lanfranchi<sup>c</sup>, J. Lee-Franzini<sup>c,m</sup>, D. Leone<sup>j</sup>, F. Lu<sup>b,c</sup>,  
M. Martemianov<sup>c,f</sup>, M. Matsyuk<sup>c,f</sup>, W. Mei<sup>c</sup>, A. Menicucci<sup>k</sup>, L. Merola<sup>g</sup>, R. Messi<sup>k</sup>, S. Miscetti<sup>c</sup>,  
M. Moulson<sup>c</sup>, S. Müller<sup>d</sup>, F. Murtas<sup>c</sup>, M. Napolitano<sup>g</sup>, A. Nedosekin<sup>c</sup>, M. Palutan<sup>l</sup>, L. Paoluzi<sup>k</sup>,  
E. Pasqualucci<sup>j</sup>, L. Passalacqua<sup>c</sup>, A. Passeri<sup>l</sup>, V. Patera<sup>c,j</sup>, E. Petrolo<sup>j</sup>, D. Picca<sup>j</sup>, G. Pirozzi<sup>g</sup>,  
L. Pontecorvo<sup>j</sup>, M. Primavera<sup>e</sup>, F. Ruggieri<sup>a</sup>, P. Santangelo<sup>c</sup>, E. Santovetti<sup>k</sup>, G. Saracino<sup>g</sup>,  
R. D. Schamberger<sup>m</sup>, B. Sciascia<sup>j</sup>, A. Sciubba<sup>c,j</sup>, F. Scuri<sup>n</sup>, I. Sfiligoi<sup>c</sup>, J. Shan<sup>c</sup>, P. Silano<sup>j</sup>,  
T. Spadaro<sup>j</sup>, E. Spiriti<sup>l</sup>, G. L. Tong<sup>b,c</sup>, L. Tortora<sup>l</sup>, E. Valente<sup>j</sup>, P. Valente<sup>c</sup>, B. Valeriani<sup>d</sup>,  
G. Venanzoni<sup>h</sup>, S. Veneziano<sup>j</sup>, A. Ventura<sup>e</sup>, Y. Wu<sup>b,c</sup>, G. Xu<sup>b,c</sup>, G. W. Yu<sup>b,c</sup>, P. F. Zema<sup>h</sup>, Y. Zhou<sup>c</sup>

<sup>a</sup>Dipartimento di Fisica dell'Università e Sezione INFN, Bari, Italy

<sup>b</sup>Institute of High Energy Physics of Academica Sinica, Beijing, China

<sup>c</sup>Laboratori Nazionali di Frascati dell'INFN, Frascati, Italy

<sup>d</sup>Institut für Experimentelle Kernphysik, Universität Karlsruhe, Germany

<sup>e</sup>Dipartimento di Fisica dell'Università e Sezione INFN, Lecce, Italy

<sup>f</sup>Institute for Theoretical and Experimental Physics, Moscow, Russia

<sup>g</sup>Dipartimento di Scienze Fisiche dell'Università e Sezione INFN, Napoli, Italy

<sup>h</sup>Dipartimento di Fisica dell'Università e Sezione INFN, Pisa, Italy

<sup>j</sup>Dipartimento di Fisica dell'Università "La Sapienza" e Sezione INFN, Roma, Italy

<sup>k</sup>Dipartimento di Fisica dell'Università "Tor Vergata" e Sezione INFN, Roma, Italy

<sup>l</sup>Dipartimento di Fisica dell'Università "Roma Tre" e Sezione INFN, Roma, Italy

<sup>m</sup>Physics Department, State University of New York at Stony Brook, USA

<sup>n</sup>Dipartimento di Fisica dell'Università e Sezione INFN, Trieste, Italy

<sup>o</sup>Physics Department, University of Virginia, USA

### Abstract

We present a study of the reaction  $e^+e^- \rightarrow \pi^+\pi^-\gamma$  at the  $\phi$  peak with the KLOE detector at the  $\phi$ -factory DAΦNE. This reaction allows us to obtain the cross section for

$e^+e^- \rightarrow \pi^+\pi^-$  from the  $e^+e^-$  center-of-mass energy  $W = m_\phi = 1019$  MeV down to threshold, i.e.  $2m_\pi < M_{\pi\pi} < m_\phi$ . This is called radiative return. The status of the analysis and preliminary results on the invariant mass spectrum of the two-pion-state are presented.

# 1 INTRODUCTION

## 1.1 Motivation

The recent surprising results of the  $g - 2$  BNL experiment [1] and the apparent large discrepancy with expectation, about three times as large as the electroweak correction, has renewed the interest in good measurements of the cross section  $e^+e^- \rightarrow \text{hadrons}$ . The corrections to the photon propagator due to low mass hadronic states cannot be computed, because QCD is not tractable in this energy regime. It is however well known that the correction to the muon anomaly,  $a_\mu$ , can be related to  $\sigma(e^+e^- \rightarrow \text{hadrons})$  by a dispersion integral. The error on  $a_\mu(\text{hadr})$  is in fact dominated by the knowledge of the hadronic cross section, or equivalently  $\tau$ -decay data. Quoted values for  $a_\mu(\text{hadr})$  are  $(6924 \pm 62) \times 10^{-11}$  ([2], using  $\tau$  data) and  $(6974 \pm 105) \times 10^{-11}$  ([3], using  $e^+e^-$  data only). Taking the evaluation of Ref. [2], theory and experiment differ by  $(426 \pm 165) \times 10^{-11}$ .

## 1.2 Radiative Return

We discuss here a method to obtain  $\sigma(e^+e^- \rightarrow \text{hadrons})$ , which employs the radiative process  $e^+e^- \rightarrow \text{hadrons} + \gamma$ , where the photon has been radiated by one of the initial electrons (positrons). This is referred to as initial state radiation or ISR [4], [5]. DAΦNE typically operates at a fixed center-of-mass energy  $W = m_\phi$ . By measuring the radiative (return) process above, the hadronic cross section becomes accessible over the mass range  $2m_\pi < M_{\pi\pi} < m_\phi$ . The cross section  $d\sigma(e^+e^- \rightarrow \text{hadrons})/ds$  can be obtained from the measurement of  $d\sigma(e^+e^- \rightarrow \text{hadrons} + \gamma)/ds$ ,  $s = W^2 = M_{\text{hadr}}^2$ . The relation is given by the radiation function  $H$  defined by:

$$s \frac{d\sigma(\text{hadrons} + \gamma)}{ds} = \sigma(\text{hadrons}) \times H(s, \theta_\gamma) \quad (1)$$

The function  $H(s, \theta_\gamma)$  (which depends also on the polar angle of the photon  $\theta_\gamma$ ) needs to be known to an accuracy better than 1%. Radiative corrections have been computed so far by different groups up to next-to-leading-order for the exclusive hadronic state  $\pi^+\pi^-$  [5], [6], [7], [8]. We concentrated in the following on the process  $e^+e^- \rightarrow \rho\gamma \rightarrow \pi^+\pi^-\gamma$ , which dominates the cross section below 1 GeV. This channel accounts for 62% of the hadronic contribution to  $a_\mu$ . We also limit our discussion to events where the photon is emitted at small angle to the beams,  $0.934 < \cos\theta_\gamma < 0.995$  ( $5^\circ < \theta_\gamma < 21^\circ$ ) and is thus unobserved. Since the event kinematics is only once constrained, large background appears at low  $M_{\pi\pi}$  due to  $\pi^+\pi^-\pi^0$  and to  $\mu^+\mu^-\gamma$  events, both having a cross section larger than  $\pi^+\pi^-\gamma$ . We have also begun using large angle photon events, where the kinematics is 4 times over constrained, three times if we ignore the  $E_\gamma$  measurement. The analysis of this channel is in a less advanced state but is the best way for studying the low dipion mass region, which is however very important for

the determination of  $a_\mu$ .

The radiative return method has one important advantage over an energy scan. The systematics of the measurement (e.g. normalization, beam energy) have to be taken into account only *once* while for the energy scan they have to be known for *each* energy point.

## 1.3 Final state radiation

Final state radiation from pions is an intrinsic background, different from background processes such as muon pairs, machine background etc. and must be distinguished from ISR. It is in general possible to correctly extract the relevant  $\pi^+\pi^-\gamma$  contribution from the FSR background with a fit to the data of the cross section for both processes, after proper folding of the detector response. In the following we suppress FSR events by kinematic cuts, which reduce this background to an acceptable limit.

Monte Carlo simulations[10] show, that cutting on  $E_\gamma = (m_\phi - E_+ - E_-)$  and  $\theta_\gamma$ , the energy and polar angle of the photon in the  $e^+e^-$  system, effectively suppresses FSR, while most of the ISR events are retained. ISR events are peaked at large  $\cos\theta_\gamma$ , while FSR photons tend to be emitted along the pion direction  $\propto \sin^2\theta_\pi$ .

A cut on  $E_\gamma$  additionally suppresses FSR due to the fact that the decay via the  $\rho$  resonance (i.e. ISR) leads to an enhancement of the photon energy spectrum at  $\approx 220$  MeV at which value FSR is very suppressed. The cuts used in the analysis given below reduce FSR to less than 1%:

$$0.934 < \cos\theta_\gamma < 0.996 \quad (2)$$

$$E_\gamma > 10 \text{ MeV} \quad (3)$$

$$55^\circ < \theta_\pi < 125^\circ \quad (4)$$

$$p_{\perp,\pi} > 200 \text{ MeV}/c \quad (5)$$

The effective cross section with these acceptance cuts is 4.2 nb. Note that, from the experimental point of view, it would be much easier to perform an analysis with no lower boundary for  $\theta_\gamma$  ( $0^\circ < \theta_\gamma < 21^\circ$ ). This would increase the cross section by a factor  $\simeq 4$  and would eliminate a detector resolution effect due to the lower angular cut. However, this is not correct in the current version of the generator, which diverges for  $\theta_\gamma \rightarrow 0^\circ$ . A new calculation with the NLO QED corrections taken into account has recently been published[7] and a new version of the generator will soon be available. This will allow to remove the lower angular cut improving the statistical error and removing a possible source of systematics.

The description of FSR is model dependent and in the actual version of Ref. [5] a point like pion is assumed. The model dependence can be tested for  $\pi^+\pi^-\gamma$  events by looking at the charge asymmetry of the produced pions:

$$A(\theta_\pi) = \frac{N^{\pi^+}(\theta_\pi) - N^{\pi^-}(\theta_\pi)}{N^{\pi^+}(\theta_\pi) + N^{\pi^-}(\theta_\pi)} \quad (6)$$

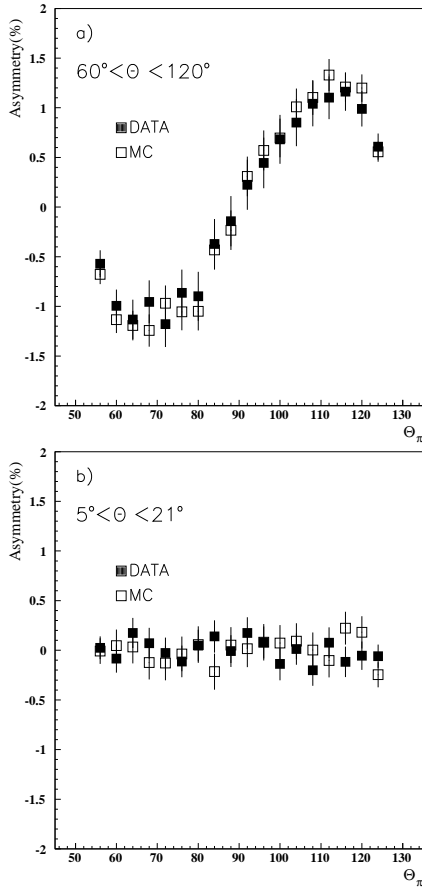


Figure 1: The charge asymmetry (formula (6)) is shown for 2 angular regions of the photon polar angle: (a)  $60^\circ < \theta_\gamma < 120^\circ$ , where we see a sizable effect of the charge asymmetry due to larger FSR and (b)  $5^\circ < \theta_\gamma < 21^\circ$ , where FSR and hence the charge asymmetry are small.

This charge asymmetry arises from the interference between ISR and FSR and is therefore linear in the FSR amplitude. We measured the charge asymmetry for (a) large photon angles ( $60^\circ < \theta_\gamma < 120^\circ$ ), where FSR is large, and (b) for small photon angles ( $5^\circ < \theta_\gamma < 21^\circ$ ). The results are illustrated in figure (1) and show very good agreement between data and Monte Carlo, indicating that the point like model describes well the process of FSR within the error bars.

#### 1.4 Studying the Pion Form Factor at threshold

For the selection cuts described above (small angle region), the ISR cross section around the  $\rho$  peak is highest, but the  $M_{\pi\pi}^2$  region at threshold is suppressed by the kinematical cuts. To avoid this, a second angular region has been defined in which we can explore the invariant mass spectrum down to  $\sqrt{M_{\pi\pi}^2} \simeq 300$  MeV:

$$0 < \cos \theta_\gamma < 0.5 \quad (7)$$

$$E_\gamma > 10 \text{ MeV} \quad (8)$$

$$55^\circ < \theta_\pi < 125^\circ \quad (9)$$

$$p_{\perp, \pi} > 200 \text{ MeV}/c \quad (10)$$

As discussed above, FSR is in average much higher at large values of  $\theta_\gamma$ , but does not play a role anymore for small values of  $M_{\pi\pi}^2$ , which we actually want to study with these new cuts.

## 2 EVENT SELECTION

In this chapter we present the event selection for the measurement of the  $\pi^+\pi^-\gamma$  final state. After a very brief description of the KLOE detector, the selection algorithm for this signal is presented.

### 2.1 The KLOE detector

KLOE [11] is a typical  $e^+e^-$  multiple purpose detector with cylindrical geometry, consisting of a large helium based drift chamber (DC, [12]), surrounded by an electromagnetic calorimeter (EmC, [13]) and a superconducting magnet ( $B = 0.6$  T). The detector has been designed for the measurement of  $CP$  violation in the neutral kaon system, i.e. for precise detection of the decay products of  $K_S$  and  $K_L$ . These are low momenta charged tracks ( $\pi^\pm, \mu^\pm, e^\pm$  with a momentum range from 150 MeV/c to 270 MeV/c) and low energy photons (down to 20 MeV).

The DC dimensions (3.3 m length, 2 m radius), the drift cell shapes (2x2 cm<sup>2</sup> cells for the inner 12 layers, 3x3 cm<sup>2</sup> cells for the outer 46 layers) and the choice of the gas mixture (90% Helium, 10% Isobutane;  $X_0 = 900$  m) had to be optimized for the requirements prevailing at a  $\phi$  factory. The KLOE design results in a very good momentum resolution:  $\sigma_{p_\perp}/p_\perp \leq 0.3\%$  at high tracking efficiencies ( $> 99\%$ ).

The EmC is made of a matrix of scintillating fibres embedded in lead, which guarantees a good energy resolution  $\sigma_E/E = 5.7\%/\sqrt{E(\text{GeV})}$  and excellent timing resolution  $\sigma_t = 57\text{ps}/\sqrt{E(\text{GeV})} \oplus 50$  ps. The EmC consists of a barrel and two endcaps which are surrounding the cylindrical DC; this gives a hermetic coverage of the solid angle (98%). However, the acceptance of the EmC below  $\approx 20^\circ$  is reduced due to the presence of quadrupole magnets close to the interaction point and does not allow to measure e.g. the photon of  $\pi^+\pi^-\gamma$  events with low  $\theta_\gamma$  angles (as required for FSR suppression).

It will be shown in the following, that an efficient selection of the  $\pi^+\pi^-\gamma$  signal is possible, without requiring an explicit photon detection. The relatively simple signature of the signal (2 high momentum tracks from the interaction point) and the good momentum resolution of the KLOE tracking detector allow us to perform such a selection.

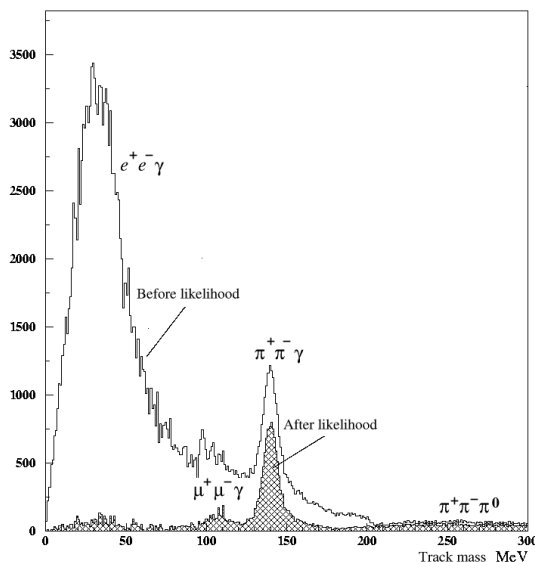


Figure 2: A likelihood method has been developed to separate electrons from pions. The kinematic variable track mass before and after the application of this method is shown.  $\pi^+\pi^-\gamma$  events are peaked at  $M_{Track} = m_\pi$ , radiative Bhabha events at much smaller values. Other background channels are also visible ( $\mu^+\mu^-\gamma$  and  $\pi^+\pi^-\pi^0$ ).

## 2.2 Selection Algorithm

The  $\pi^+\pi^-\gamma$  events are selected using the following 4 steps. The selection is based on the measurement of the charged pion tracks by the DC, while the photon is not required to be detected in the EmC. Calorimeter information is however used for the  $\pi/e$ -separation (likelihood method).

i) Charged vertex in DC. We require 1 vertex in the DC with 2 associated charged tracks close to the interaction point:  $\sqrt{(x_V^2 + y_V^2)} \leq 8$  cm and  $|z_V| \leq 15$  cm.

ii) Likelihood Method for  $\pi/e$ -separation. A fraction of radiative Bhabha events  $e^+e^-\gamma$  enters the kinematical selection (see next selection cut), giving rise to a non negligible background. In order to reject those events, a likelihood method has been worked out for an effective  $\pi/e$ -separation. The method is based on the shape and energy deposition of the EmC clusters produced by the charged tracks and has been developed using independent control samples for the pion information ( $\pi^+\pi^-\pi^0$  events) and for the electron information ( $e^+e^-\gamma$  events). 98% of all  $\pi^+\pi^-\gamma$  events are selected if at least one of the two tracks has been identified as a pion by the likelihood method. In figure (2) the effect of the likelihood method is demonstrated in the track mass ( $M_{Track}$ ) distribution<sup>1</sup>.  $\pi^+\pi^-\gamma$  events are peaked at  $M_{Track} = m_\pi$ , radiative Bhabha events at smaller values.

iii) Kinematic Cut:  $130.2 \text{ MeV} < M_{Track} < 149.0 \text{ MeV}$ . We perform a  $\pm 9.6 \text{ MeV}$  ( $\pm 2\sigma$ ) cut on the kinematical variable  $M_{Track}$ , which is peaked at

<sup>1</sup>The  $M_{Track}$  variable is obtained applying the 4-momentum-conservation and resolving it for the particle mass.

$M_{Track} = m_\pi$  for  $\pi^+\pi^-\gamma$  events (see figure (2)). Background of  $\pi^+\pi^-\pi^0$  events (with  $M_{Track}$  mostly  $> 150$  MeV),  $\mu^+\mu^-\gamma$  (with  $M_{Track}$  peaked at  $m_\mu$ ) and the bulk part of radiative Bhabha events  $e^+e^-\gamma$  ( $M_{Track} < 100$  MeV) are mostly rejected (see subchapter 3.1 on background). This cut assumes a  $\pi^+\pi^-\gamma$  final state.

iv) Acceptance Cuts. The missing momentum of the 2 accepted charged tracks is calculated and associated with the photon under the assumption of a  $\pi^+\pi^-\gamma$  event:  $\vec{p}_\gamma = \vec{p}_\phi - \vec{p}_+ - \vec{p}_-^2$ . The acceptance cuts of formulae (2)-(5) are then applied.

## 3 EVENT ANALYSIS

The  $\pi^+\pi^-\gamma$  cross section measurement contains the following terms:

$$\frac{d\sigma_{\text{hadrons}+\gamma}}{dM_{\pi\pi}^2} = \frac{dN_{\text{Obs}} - dN_{\text{Bkg}}}{dM_{\pi\pi}^2} \frac{1}{\epsilon_{\text{Sel}}\epsilon_{\text{Acc}}} \frac{1}{\int \mathcal{L} dt} \quad (11)$$

It requires the study of the various background channels ( $N_{\text{Bkg}}$ , see following subchapter), the selection efficiencies ( $\epsilon_{\text{Sel}}$ ) and the systematic effects due to the acceptance cuts applied ( $\epsilon_{\text{Acc}}$ ). Finally the counting rate measurement has to be normalized to the integrated luminosity  $\int \mathcal{L} dt$  in order to achieve a cross section measurement. All these terms will be obtained from data for the final analysis.

Preliminary results concerning  $\epsilon_{\text{Sel}}$  are presented in the following subchapter. The detector resolution and the systematic effects, arising from there have been studied in detail with MC [10]. No limitations have been found for a high precision measurement at the percent level.

<sup>2</sup> $\vec{p}_\phi$  is the  $\phi$  momentum in the laboratory system due to the beam crossing angle.

### 3.1 Background

$$e^+e^- \gamma, \mu^+\mu^- \gamma$$

Radiative Bhabha events are mostly suppressed by the  $M_{Track}$  cut (chapter 2.2 (ii)). The remaining background due to events with a high value for  $M_{Track}$  and due to electrons, which have not been rejected by the likelihood method, is peaked at large  $M_{\pi\pi}^2$  (above  $0.7 \text{ GeV}^2$ ) and corresponds to a contamination below the percent level in this  $M_{\pi\pi}^2$  region.

$\mu^+\mu^- \gamma$  events are not efficiently rejected by the likelihood method, because they release a pattern in the EmC with a signature similar to pions. After the cuts of formulae (2) - (5) and after the  $M_{Track}$  cut, the remaining  $\mu^+\mu^-$  cross section is low ( $\approx 10^{-2} \text{ nb}$ ), such that we expect only a small contamination ( $< 1\%$  in the high  $M_{\pi\pi}^2$  region  $> 0.7 \text{ GeV}^2$ ).

$$\pi^+\pi^-\pi^0$$

An important background for our signal is the decay  $\phi \rightarrow \pi^+\pi^-\pi^0$  (B.R. 15.5%,  $\sigma_{\pi^+\pi^-\pi^0}^{tot} \approx 500 \text{ nb}$ ).  $\pi^+\pi^-\pi^0$  and  $\pi^+\pi^-\gamma$  events are separated in the KLOE standard reconstruction scheme by a cut in the 2-dimensional plane  $M_{Track} - M_{\pi\pi}^2$ . At small  $M_{\pi\pi}^2$ , the  $M_{Track}$  values for the 2 channels are very similar and a part of the  $\pi^+\pi^-\pi^0$  events appear as background. The  $M_{Track}$  cut and the acceptance cut of formula (5)<sup>3</sup> reject a big part of these events.

In order to estimate from data the remaining contamination, we modified the standard cut in the  $M_{Track} - M_{\pi\pi}^2$  plane by expanding the  $\pi^+\pi^-\pi^0$  selection region. We see then the tail of  $\pi^+\pi^-\pi^0$  events entering the  $M_{Track}$  selection interval. We perform this study in bins of  $M_{\pi\pi}^2$ . The  $\pi^+\pi^-\pi^0$  background is negligible in most of the  $M_{\pi\pi}^2$  region and gives only a contamination at the lower end of the spectrum between  $0.3 \text{ GeV}^2$  and  $0.4 \text{ GeV}^2$ . The effective  $\pi^+\pi^-\pi^0$  cross section after all the selection steps is  $< 0.01 \text{ nb}$ . It increases considerably if we select  $\pi^+\pi^-\gamma$  events at larger polar angles of the photon<sup>4</sup>

### 3.2 Selection Efficiencies

We shortly summarize the various efficiencies which contribute to the total selection efficiency:

- **Trigger:** The trigger efficiency has 2 contributions: the probability of a  $\pi^+\pi^-\gamma$  event to be recognized by the KLOE trigger (between 95% to 99% depending on  $M_{\pi\pi}^2$ ) and the inefficiency which arises from a trigger hardware veto for the filtering of cosmic ray events. The second contribution causes an inefficiency for  $\pi^+\pi^-\gamma$  events at large  $M_{\pi\pi}^2$  (30% at  $1 \text{ GeV}^2$ ) which decreases with lower  $M_{\pi\pi}^2$  (fully efficient at  $\approx 0.7 \text{ GeV}^2$ ). These values have been obtained from

<sup>3</sup>The pion tracks have on the average a lower momentum as  $\pi^+\pi^-\gamma$  events.

<sup>4</sup>This behaviour can be easily explained by the missing momentum of  $\pi^+\pi^-\pi^0$  events (in this case the  $\pi^0$ ), which is peaked at large angles.

data by looking at the individual probabilities for  $\pi^+$  and  $\pi^-$  to fire 1 trigger sector and 1 cosmic veto sector.

- **Reconstruction Filter:** A software filter is implemented in the KLOE reconstruction program for the filtering of non-collider physics events, like e.g. machine background and cosmic ray events. The inefficiency for  $\pi^+\pi^-\gamma$  events caused by this filter is  $\approx 2\%$  (taken from MC).
- **Event Selection** (see subchapter 2.2): The DC vertex efficiency ( $\approx 95\%$ ) is obtained from Bhabha events, selected without requiring DC information. The efficiency due to the likelihood selection is  $\approx 98\%$  and is evaluated from data during the construction of the likelihood method. The efficiency due to the  $M_{Track}$  cut ( $\approx 90\%$ ) is evaluated from Monte Carlo at present.

### 3.3 Luminosity Measurement

The DAΦNE luminosity is measured by KLOE using large angle Bhabha (LAB) events. The effective Bhabha cross section at large angles ( $55^\circ < \theta_{+,-} < 125^\circ$ ) is still as high as  $425 \text{ nb}$ . The number of LAB candidates  $N_{LAB}$  are counted and normalized to the effective Bhabha cross section, obtained from Monte Carlo:

$$\int \mathcal{L} dt = \frac{N_{LAB}(\theta_{+,-})}{\sigma_{LAB}^{MC}(\theta_{+,-})} \cdot (1 - \delta_{Bkg}) \quad (12)$$

Hence, the precision of this measurement depends on: (i) the theoretical knowledge of the Bhabha scattering process including radiative corrections; (ii) the simulation of the process by the detector simulation program.

For the theory part we are using 2 independent Bhabha event generators: the Berends-Kleiss [14] generator, modified for DAΦNE in [15] and the BABAYAGA generator[16].

We use a selection algorithm for LAB events with a reduced number of cuts, for which we expect a very good description by the KLOE detector simulation program. The acceptance region for the electron and positron polar angle ( $55^\circ < \theta_{+,-} < 125^\circ$ ) is measured by the EmC clusters produced by these tracks, while the energy measurement ( $E_{+,-} > 400 \text{ MeV}$ ) is performed by the high resolution drift chamber. Taking the actual detector resolutions, we expect the systematic errors arising from these cuts to be well below 1%. Background from  $\mu^+\mu^- (\gamma)$ ,  $\pi^+\pi^-\gamma$  and  $\pi^+\pi^-\pi^0$  is below 1% and can be easily subtracted. All the selection efficiencies concerning the LAB measurement (Trigger, EmC cluster, DC tracking) are above 98% and are well reproduced by the detector simulation.

As a goal we expect to measure the DAΦNE luminosity at the level of 1%. The very good agreement of the experimental distributions ( $\theta_{+,-}$ ,  $E_{+,-}$ ) with the existing

event generators and a cross check with an independent luminosity counter based on  $e^+e^- \rightarrow \gamma\gamma(\gamma)$ , indicate a good accuracy. However, more systematic checks (e.g. the effect of a varying beam energy and of a non centered beam interaction point) are still to be done.

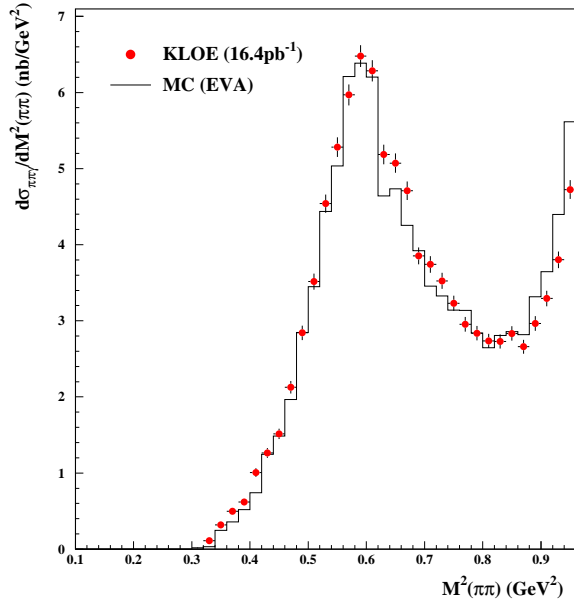


Figure 3: The differential  $\pi^+\pi^-\gamma$  cross section as a function of the pion invariant mass. The solid line is the prediction of the theoretical event generator EVA of Ref. [5].

### 3.4 Comparison with Monte Carlo

We analyzed a data sample of  $16.4 \text{ pb}^{-1}$  and present in figure 3 the preliminary result for the dipion invariant mass spectrum  $M_{\pi\pi}^2$  (small angle region) and in figure 4 the pion form factor  $|F_\pi|^2$ . Therefore we applied formula (1) and write for  $\sigma_{\text{hadrons}} = \pi\alpha^2\beta_\pi^3/(3M_{\pi\pi}^2) \times |F_\pi(M_{\pi\pi}^2)|^2$ . In plot 4 both the small angle (formulae (2)-(5)) and the large angle events (formulae (7)-(10)) are plotted. The solid line is a Gounaris-Sakurai parametrization with a fixed set of parameters and allows a qualitative comparison with data. No attempt has been made to subtract the residual contribution of  $\phi \rightarrow \pi^+\pi^-\pi^0$  events which are present at low  $M_{\pi\pi}^2$ .

The statistical error of the data points in the  $\rho$  peak region is  $\approx 2\%$ . The actual version of the event generator has a systematic uncertainty of the same size. By comparing the data and MC distributions we conclude that the accuracy of our cross section measurement is at the level of a few percent, which will be considerably improved with the ongoing analysis.

## 4 SUMMARY AND OUTLOOK

We presented in this paper a preliminary measurement  $d\sigma(e^+e^- \rightarrow \pi^+\pi^-\gamma)/dM_{\pi\pi}^2$  for  $M_{\pi\pi}^2 < 1 \text{ GeV}^2$ , using

the radiative return method. The data sample<sup>5</sup>, corresponding to an integrated luminosity of  $16.4 \text{ pb}^{-1}$  shows a good agreement with the “standard” parametrization for the  $\rho$  peak. It also shows the possibility for KLOE of exploring the hadronic cross section at threshold. We conclude that the experimental understanding of efficiencies, background and luminosity are well under control. We further conclude that the radiative return is a competitive method to measure hadronic cross sections. We note again the advantage of the radiative return. Systematic errors, like luminosity and beam energy, enter only globally and do not have to be known for individual energy points.

For the future we plan to refine the analysis and to include very small angle photons. A comparison with MC will be possible in this case with the new next-to-leading-order event generator [7] and will improve the precision of the measurement due to a better systematic control of the fiducial volume. Moreover we are studying the possibility to enlarge the acceptance region for  $\theta_{+,-}$ , which increases the kinematical acceptance of events at low  $M_{\pi\pi}^2$ ,  $< 0.3 \text{ GeV}^2$ . In order to improve on the accuracy of  $a_\mu(\text{hadr})$  and to be competitive with results coming from the CMD-2 experiment in Novosibirsk [17], a final precision for this measurement below 1% is needed. A statistical error on this level can be obtained with an integrated luminosity of  $\sim 200 \text{ pb}^{-1}$  which could be collected before year end. DAΦNE has recently achieved a luminosity  $\mathcal{L} > 1.5 \text{ pb}^{-1} \text{ d}^{-1}$ .

We are also studying how to measure  $d\sigma(e^+e^- \rightarrow \pi^+\pi^- + n\gamma)/dM_{\pi\pi}^2$ , which simply means choosing events which satisfy appropriate kinematical constraints to reject unwanted backgrounds and then apply precise transverse momentum and energy unbalance for proper inclusion of soft photons, to facilitate computation of the physical cross section. The radiative corrections for such a measurement are obtainable with high precision ( $< 0.5\%$ )[9].

At low energy,  $M_{\pi\pi} < 600 \text{ MeV}$ , the  $\mu^+\mu^-\gamma$  cross section becomes larger than the dipion cross section. It therefore becomes possible to measure the ratio  $\sigma_{\pi^+\pi^-\gamma}/\sigma_{\mu^+\mu^-\gamma}$  in which initial state radiation and vacuum polarization effects cancel. Final state radiation corrections are still necessary. On the experimental side one needs only to estimate the difference in the efficiency for the two channels rather than the entire efficiency.

## 5 ACKNOWLEDGEMENT

We would like to thank F. Jegerlehner, J.H. Kühn, G. Rodrigo and W. Marciano for the very useful discussions and critical remarks during the preparation and the analysis of this measurement.

## 6 REFERENCES

<sup>5</sup> This corresponds to about one half of the full data set which KLOE has taken in 2000.

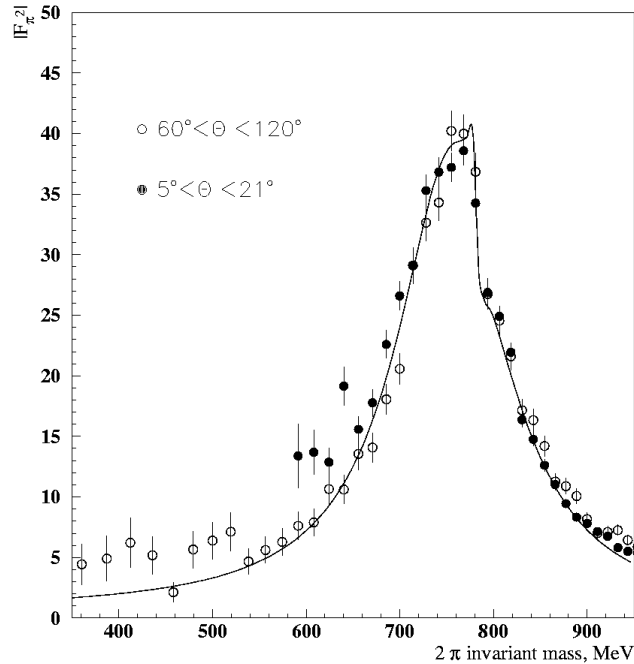


Figure 4: The pion form factor as a function of the  $\sqrt{s}$  of the hadronic system for small and large angles. The line is a Gounaris-Sakurai parametrization with fixed parameters. No fit has been attempted.

- [1] H.N. Brown *et al.* [E821 collaboration], *Phys.Rev.Lett.* **86** (2001) 2227
- [2] M. Davier and A. Höcker, *Phys.Lett. B* **435** (1998) 427
- [3] F. Jegerlehner, [hep-ph/0104304]
- [4] S. Spagnolo, *Eur. Phys. J. C* **6** (1999) 637
- [5] S. Binner, J.H. Kühn, K. Melnikov, *Phys.Lett. B* **459** (1999) 279
- [6] V.A. Khoze, M.I. Konchatnij, N.P. Merenkov, G. Pancheri, L. Trentadue, O.N. Shekhoviyova, *Eur. Phys. J. C* **18** (2001) 481
- [7] G. Rodrigo, A. Gehrmann-De Ridder, M. Guillaume, J.H. Kühn, [hep-ph/0106132]
- [8] K. Melnikov, F. Nguyen, B. Valeriani, G. Venanzoni, *Phys.Lett. B* **477** (2000) 114
- [9] A. Höfer, J. Gluza and F. Jegerlehner, *Pion Pair Production with Higher Order Radiative Corrections in Low Energy  $e^+e^-$  Collisions*, **DESY-00-163** (2001)
- [10] A.Denig, Proceedings to *DAΦNE'99, Frascati Physics Series XVI* (2000) 569
- [11] A. Aloisio *et al.* [KLOE collaboration], *The KLOE Detetor, Technical Proposal*, **LNF-93/002** (1993)
- [12] M. Adinolfi *et al.* [KLOE collaboration], *The Tracking Detector of the KLOE Experiment*, **LNF-01/016** (2001); to be published in *Nuclear Instruments and Methods*
- [13] M. Adinolfi *et al.* [KLOE collaboration], *The KLOE electromagnetic calorimeter*, **LNF-01/017** (2001); to be published in *Nuclear Instruments and Methods*
- [14] F.A. Berends, R. Kleiss, *Nucl.Phys. B* **228** (1988) 537
- [15] E. Drago, G. Venanzoni, *A Bhabha Generator for DAΦNE including radiative corrections and  $\phi$  resonance*, **INFN/AE-97/48** (1997)
- [16] C.M.C. Calame, C. Lunardini, G. Montagna, O. Nicosini, F. Piccinini, *Nucl.Phys. B* **584** (2000) 459
- [17] R.R. Akhmetshin *et al.* [CMD-2 collaboration], [hep-ex/9904027]